Inorganic Chemistry

Article

pubs.acs.org/IC

Guanine Nucleobase Adducts Formed by [Pt(di-(2-picolyl)amine)Cl]Cl: Evidence That a Tridentate Ligand with Only in-Plane Bulk Can Slow Guanine Base Rotation

Chase Andrepont, Patricia A. Marzilli, and Luigi G. Marzilli*

Department of Chemistry, Louisiana State University, Baton Rouge, Louisiana 70803, United States

Supporting Information

ABSTRACT: Pt(II) complexes bind preferentially at N7 of G residues of DNA, causing DNA structural distortions associated with anticancer activity. Some distortions induced by difunctional cisplatin are also found for monofunctional Pt(II) complexes with carrier ligands having bulk projecting toward the guanine base. This ligand bulk can be correlated with impeded rotation about the Pt−N7(guanine) bond. Pt(*N*(H)dpa)(**G**) adducts (*N*(H)dpa = di-(2-picolyl)amine, **G** = 5′-GMP, 5′-GDP, 5′-GTP, guanosine, 9-EtG, and 5′-IMP) were used to assess whether a tridentate carrier ligand having bulk concentrated in the coordination plane can impede guanine nucleobase rotation. Because the Pt(*N*(H)dpa) moiety contains a mirror plane but is unsymmetrical with respect to the coordination plane, Pt(*N*(H)dpa)(**G**) adducts can form anti or syn rotamers with the guanine O6 and the central N−H of *N*(H)dpa on the opposite or the same side of the coordination plane, respectively. The observation of two sharp, comparably intense guanine H8 NMR signals provided evidence that these Pt(*N*(H)dpa)(**G**) adducts exist as mixtures of syn and anti rotamers, that rotational interchange is impeded by *N*(H)dpa, and that the key interactions involves steric repulsions between the pyridyl and guanine rings. The relative proximity of the guanine H8 to the anisotropic pyridyl rings allowed us to conclude that the syn rotamer was usually more abundant. However, the anti rotamer was more abundant for the Pt(*N*(H)dpa)(5′-GTP) adduct, in which a hydrogen bond between the 5′-GTP γ-phosphate group and the *N*(H)dpa central N−H is geometrically possible. In all previous examples of the influence of hydrogen bond formation on rotamer abundance in Pt(II) guanine adducts, these hydrogen bonding interactions occurred between ligand groups in cis positions. Thus, the role of a trans ligand group in influencing rotamer abundance, as found here, is unusual.

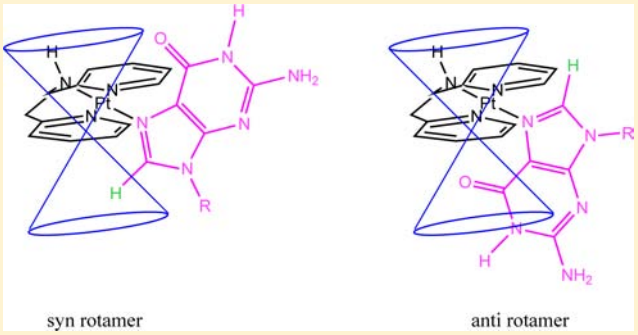

INTRODUCTION

Cisplatin (*cis*-Pt(NH$_3$)$_2$Cl$_2$) and related difunctional PtLX$_2$ analogues (L = one bidentate or two *cis*-unidentate N-donors, X$_2$ = anionic leaving groups) are among the most widely studied anticancer agents.[1−11] DNA is generally accepted as the primary target.[12,13] Difunctional Pt drugs attack G N7 of adjacent G residues, forming a G*G* intrastrand cross-link lesion.[4,6,14−17] G residues in DNA or oligomers with a Pt(II) center bound to N7 are designated as G*. Intense interest over many years focused on the distortions caused in the G*G* base pair (bp) step, namely, the relationship of the 5′-G*•C bp to the 3′-G*•C bp.[12] However, more recent developments have shown that another bp step could be even more distorted. X-ray studies of an HMG-bound 16-mer duplex in the solid state,[18] and a subsequent X-ray/NMR-derived model of a 9-mer duplex in solution,[19] both containing an intrastrand cisplatin lesion, revealed an unusual XG* bp step. The distortion involving the X•Y bp adjacent to the 5′-G*•C bp in the 5′-direction along the duplex (referred to as the Lippard bp step)[20] is characterized by a large positive shift and a large positive slide. X-ray studies of an oligomer adduct of a rather bulky monofunctional Pt anticancer agent have revealed a similar shift and slide of the XG* bp step involving the X•Y bp that is adjacent to the 5′-G*•C bp in the 5′-direction along the duplex.[21,22] For a difunctional agent, when L is bulky, activity decreases and toxicity increases.[23−27] However, for a monofunctional Pt(II) agent, the opposite situation may hold true: greater ligand bulk appears to be correlated with enhanced activity.[12,21,22,28]

In simple Pt(L)(**G**) [tridentate L] or Pt(L)(**G**)$_2$ [bidentate L] adducts (boldface **G** is an N9 guanine or N9 hypoxanthine derivative not linked to another nucleobase, Figure 1), the nucleobase orients roughly perpendicular to the coordination plane (defined by the Pt and the four ligating atoms of the pseudo square planar complexes, Figure 2). In Pt(II) adducts with DNA, the G* nucleobase orientation is strongly influenced by a combination of the DNA structure and the steric interactions of the nucleobase with the carrier ligand.[29,30] Considerable effort has been expended in studying Pt(L)(**G**)$_2$ models and in comparing results to related G*G* intrastrand models with short oligonucleotides.[12,20,29,31−33] Both model

Received: August 26, 2012
Published: October 24, 2012

   dx.doi.org/10.1021/ic3018634 | *Inorg. Chem.* 2012, 51, 11961−11970

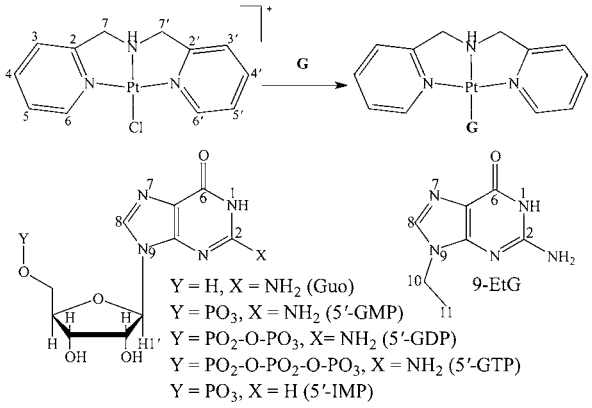

Figure 1. Adduct formation reactions of $[Pt(N(H)dpa)Cl]^+$ with various purine derivatives.

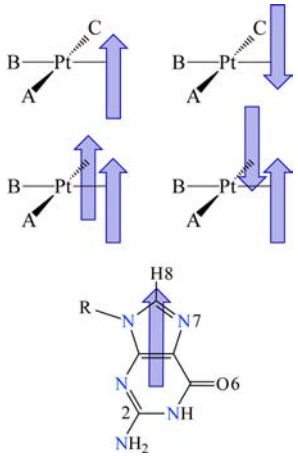

Figure 2. Possible rotamers for mono and cis bis Pt(II) adducts of purine ligands illustrated using guanine nucleobase N9 derivatives as an example. Note that the nucleobase is represented by an arrow with the tip at the H8 of the purine. For the monoadducts (top two drawings), both possible base orientations (arrow up and arrow down) lead to only one isomer if R is not chiral, A, B, and C are symmetric with respect to the coordination plane, and A = C. If A is not equal to C, the two orientations represent two rotamers. If B is not symmetric with respect to the coordination plane, then there are two rotamers regardless of whether or not A = C. The middle two drawings show the HH orientation (left) and one HT orientation (right) for cis bis Pt(II) adducts. For a given purine nucleobase derivative, as many as four rotamers are possible depending on whether or not A = B.

types can have as many as two head-to-head (HH) and two head-to-tail (HT) rotamers, depending on the bulk and symmetry of L (Figure 2).[24,29,34−39] However, the monofunctional adducts have at most one syn and one anti rotamer (Figure 2). Rotamers interconvert by rotation about the Pt−N7 bond.[19,24,40−43]

Because a key aspect of designing new Pt(II) drugs is to learn the effects of carrier-ligand bulk on the mechanism of action leading to distortion of DNA, on activity, and on toxicity,[30,36] it is important to gain a better understanding of steric effects in monofunctional adducts. One method of assessing whether a carrier ligand is bulky enough to interact with a guanine residue, thereby influencing the structure of the Pt drug DNA adduct, is to determine if **G** nucleobase rotation around the Pt−N7 bond in Pt(L)(**G**) adducts is hindered sufficiently by L to allow observation of separate sets of NMR signals for the rotamers.[17,31,35−37,40,41,43−45] The downfield **G** H8 ^{1}H NMR signals have historically been the most useful signals for assessing the presence of rotamers.[33,46−49] With a nonbulky L, rotation about the Pt−N7 bond is fast on the NMR time scale, and the single H8 NMR signal observed typically for each unique **G** represents the time average of the two guanine orientations.[43,45−48,50,51]

DNA adducts of the monofunctional complex, [Pt(dien)Cl]Cl (dien = diethylenetriamine), have been studied extensively as a "control" useful in understanding the nature of DNA binding of difunctional Pt(II) anticancer drugs.[51−56] From the data on Pt(dien)(**G**) adducts,[51] it is clear that dien is a rather small nonbulky carrier ligand. Unlike cisplatin, small monofunctional agents do not greatly disrupt the DNA structure on adduct formation; for example, minimal change in the DNA CD spectrum is caused by [Pt(dien)Cl]Cl[57] and $[Pt(NH_3)_3Cl]Cl$[58] agents. Cisplatin, in contrast, causes large CD spectral changes.[57,59,60] Likewise, evidence exists from ^{31}P NMR data on DNA adducts that the DNA structure is distorted by cis difunctional Pt agents, but not by small monofunctional Pt agents.[61,62] To assess how interactions of nucleic acid substituents (bases, phosphate groups, etc.) with a carrier ligand having in-plane bulk influence the properties of Pt(L)(**G**) adducts, we have used NMR techniques to study Pt(*N*(H)dpa)(**G**) adducts containing a tridentate carrier ligand, di-(2-picolyl)amine (*N*(H)dpa), with **G** = 5′-GMP, 5′-GDP, 5′-GTP, guanosine, 9-EtG, and 5′-IMP (Figure 1). Limited studies of Pt and Pd *N*(H)dpa complexes have shown evidence for cytotoxicity.[63,64] However, the mechanism of anticancer activity is not known.

EXPERIMENTAL SECTION

Starting Materials. $K_2[PtCl_4]$, *N*(H)dpa, guanosine (Guo), 5′-guanosine monophosphate disodium salt (5′-GMP), 5′-guanosine diphosphate sodium salt (5′-GDP), 5′-guanosine triphosphate sodium salt (5′-GTP), 5′-inosine monophosphate (5′-IMP), and 9-ethylguanine (9-EtG) were obtained from Aldrich. *cis*-$Pt(DMSO)_2Cl_2$[65] and [Pt(*N*(H)dpa)Cl]Cl[66] were synthesized as described in the literature.

NMR Measurements. NMR spectra were recorded on a 400 MHz Bruker spectrometer, typically with 10 mM samples in a D_2O/DMSO-d_6 mixture (pH adjusted with 0.5 M solutions of DCl or NaOD in D_2O). For ^{1}H NMR and ^{13}C NMR spectra in D_2O/DMSO-d_6, peak positions are referenced relative to TMS by using the signals at 2.50 ppm (residual) and 39.5 ppm, respectively, of DMSO-d_6.[67] A presaturation pulse to suppress the water peak was used when necessary. Rotating-Frame Overhauser Effect Spectroscopy (ROESY) experiments were performed at 5 °C by using a 200 ms mixing time. ^{1}H-^{13}C HSQC NMR spectra were recorded to assign the signals of the adducts. NMR data were processed with TopSpin and MestreNova software.

Pt(*N*(H)dpa)(5′-GMP) Adduct. A 28.6 mM solution of [Pt(*N*(H)-dpa)Cl]Cl in DMSO-d_6 (210 μL) was treated with a 38.5 mM solution of 5′-GMP in 390 μL of D_2O to give a 1:2.5 ratio (10 mM:25 mM) of Pt:5′-GMP, and the solution (pH ∼4) was kept at 25 °C. A solution of D_2O and DMSO-d_6 (65:35) was employed to improve the solubility of the reactants. The reaction mixture was monitored by ^{1}H NMR spectroscopy until there was no change in the bound vs free H8 signal intensity, or until the $[Pt(N(H)dpa)Cl]^+$ signals completely disappeared.

Other Pt(*N*(H)dpa)(G) Adducts. Adducts of 5′-GDP, 5′-GTP, Guo, 9-EtG, and 5′-IMP were formed in D_2O/DMSO-d_6 in a manner similar to that used for 5′-GMP. Reactions were monitored at various intervals from 10 min to 6 d by ^{1}H NMR spectroscopy as described above.

dx.doi.org/10.1021/ic3018634 | *Inorg. Chem.* 2012, 51, 11961−11970

RESULTS AND DISCUSSION

Background. Two rotamers differing with respect to the **G** base orientation (Figure 2) are conceivable for Pt(II) complexes of the type, Pt(L)(**G**), when L = a tridentate carrier ligand that is unsymmetrical with respect to the coordination plane but symmetrical about a plane perpendicular to the coordination plane. The Pt(*N*(H)dpa)(**G**) adducts fall into this category because the central N−H of the *N*(H)dpa carrier ligand projects out of the coordination plane (Figure 3). In the present study, we adopt a known stereochemical convention[44] as follows: the rotamer with the H atom of the central N−H group and the guanine O6 on the same side of the coordination plane is named syn, and the rotamer with these groups on the opposite side of this plane is named anti (Figure 3). In a study of Pt(Me_5dien)(**G**) adducts (Me_5dien = *N*,*N*,*N*′,*N*″,*N*″-pentamethyldiethylenetriamine), Carlone et al.[44] found that the Pt(Me_5dien)(5′-GMP) adduct gave two sharp H8 NMR signals ∼0.8 ppm downfield from the free 5′-GMP H8 signal. This result indicates that the adduct exists as a mixture of both possible rotamers. In contrast, Pt(dien)(**G**) adducts show only one sharp H8 signal,[51,52,56,68,69] indicating unimpeded rotation of the nucleobase, as would be expected from the low dien bulk. Thus, it is clear that the terminal dimethylamino groups of Me_5dien have enough bulk to hinder rotation of the guanine base about the Pt−N7 bond. Christoforou et al.[45] later showed that having either one or two unsubstituted terminal NH_2 groups in the tridentate carrier ligand was not sufficient to hinder **G** rotation about the Pt−N7 bond.

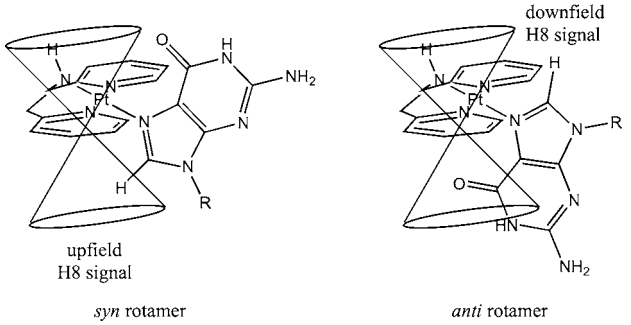

Figure 3. Two possible rotamers (syn and anti) for Pt(L)(**G**) complexes with tridentate ligands unsymmetrical with respect to the coordination plane but symmetrical about a plane perpendicular to the coordination plane are illustrated for L = *N*(H)dpa. Also illustrated are the anisotropic pyridyl rings, showing the shielding of the H8 in the syn rotamer by the pyridyl rings. This shielding results in an upfield shift of the syn H8 signal. The H8 in the anti rotamer points away from the pyridyl rings, resulting in a downfield shift of the anti H8 signal compared to the shift of the syn H8 signal.

The ^{1}H NMR spectra of all Pt(*N*(H)dpa)(**G**) adducts formed in the present study are consistent with impeded rotation of the purine nucleobase around the Pt−N7 bond. For example, the spectrum of the Pt(*N*(H)dpa)(5′-GMP) adduct shows two downfield H8 signals (Figure 4).

NMR Assignment Strategy. ^{1}H and ^{13}C NMR data and assignments for the Pt(*N*(H)dpa)(**G**) adducts and the [Pt(*N*(H)dpa)Cl]$^+$ complex are collected in Tables 1, 2, and 3. In Figure 4, the bottom trace for [Pt(*N*(H)dpa)Cl]$^+$ shows an H6/6′ signal at ∼8.6 ppm, but the spectrum of the Pt(*N*(H)dpa)(5′-GMP) adduct (top) has no doublets in this region. As discussed below, the anisotropy of the N7-coordinated guanine nucleobase shifts the H6/6′ doublets

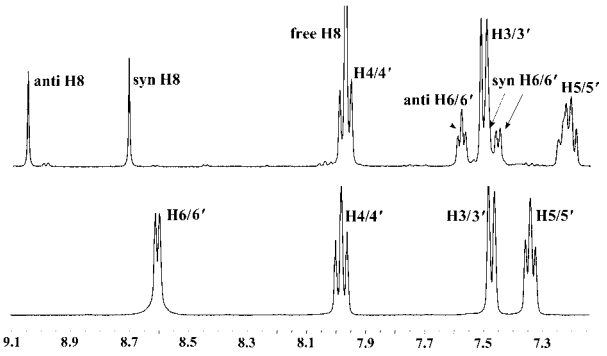

Figure 4. Aromatic region of the ^{1}H NMR spectra (25 °C, D_2O/DMSO-d_6) of [Pt(*N*(H)dpa)Cl]$^+$ (*bottom*) and the Pt(*N*(H)dpa)(5′-GMP) adduct (*top*) (shifts in ppm).

Table 1. Selected ^{1}H NMR Shifts (ppm) for G in Pt(*N*(H)dpa)(G) Adducts in D_2O/DMSO-d_6 at 25 °C

G	H8 free	H8 anti	H8 syn	H1′ free	H1′ anti	H1′ syn
9-EtG[a]	7.67	8.73	8.40			
Guo	7.91	8.95	8.61	5.71	5.93	5.85
5′-GMP[b]	7.96	9.08	8.72	5.71	5.98	5.91
5′-GDP	7.98	9.15	8.79	5.70	5.97	5.90
5′-GTP	7.97	9.21	8.79	5.70	5.98	5.91
5′-IMP[c]	8.33	9.44	9.09	5.93	6.19	6.13

[a] CH_2: 4.16 (anti), 4.05 (syn), and 3.90 ppm (free); CH_3: 1.44 (anti), 1.34 (syn), and 1.24 ppm (free). [b] H2′: 4.69 ppm, 4.53 ppm (free). [c] H2: 8.26 (syn), 8.17 (anti), and 8.05 ppm (free).

Table 2. ^{1}H NMR Shifts (ppm) and Coupling Constants (*J*, Hz) for the *N*(H)dpa Carrier Ligand in Pt(*N*(H)dpa)(G) and in [Pt(*N*(H)dpa)Cl]Cl in D_2O/DMSO-d_6 at 25 °C

Cl or G	H6/6′	H5/5′	H4/4′	H3/3′
Cl[a]	8.61 (5.8)	7.34	7.98	7.48 (8.0)
5′-GMP[b,c]	7.57[d] (5.4)	7.21	7.97 (7.8)	7.51 (8.0)
	7.51[e]			
	7.44[f] (5.4)			
5′-GDP[c]	7.58[d] (5.8)	7.23	7.98 (7.8)	7.50 (8.0)
	7.50[e]			
	7.45[f] (5.8)			
5′-GTP[c]	7.57[d] (5.8)	7.23	7.97 (7.8)	7.49 (7.8)
	7.49[e]			
	7.43[f] (5.8)			
5′-IMP[c]	7.52[g]	7.19		
	7.97 (7.9)	7.52 (7.7)		
	7.45[f] (5.6)			
	7.37[f] (5.6)			
Guo[c]	7.61[d]	7.25	8.02 (7.9)	7.54 (7.8)
	7.50[f] (5.7)			
9-EtG[c]	7.56[g]	7.25	8.02 (7.8)	7.56 (8.0)
	7.48[f] (5.4)			

[a] *J* values for H5/5′ (5.8, ∼7.7) and for H4/4′ (8.0, ∼7.7); H7/7′, *endo*-CH and *exo*-CH, respectively, 4.73 and 4.49 ppm. In DMSO-d_6, ppm (Hz): NH, 9.03; H6/6′, 8.81 (5.8); H5/5′, 7.63 (∼6.8); H4/4′, 8.24 (∼7.9); H3/3′, 7.77 (7.9); and H7/7′, *endo*-CH and *exo*-CH, respectively, 4.92 (15.9, 8.9) and 4.60 (15.9, 5.1). [b] H7/7′, *endo*-CH and *exo*-CH, respectively, 4.80 and 4.57 ppm. [c] *J* values not determined for H5/5′ because of overlap of rotamer signals, and the H4/4′ values are generally an approximate average value for coupling to H3/3′ and H5/5′. [d] anti. [e] syn, but overlapped with the H3/3′ signal. [f] syn. [g] anti, but overlapped with the H3/3′ signal.

dx.doi.org/10.1021/ic3018634 | *Inorg. Chem.* 2012, 51, 11961−11970

Table 3. ^{13}C NMR Spectral Data (ppm) for [Pt(*N*(H)dpa)Cl]Cl and the Pt(*N*(H)dpa)(5′-GMP) adduct in D_2O/DMSO-d_6 at 25 °C

carbons	[Pt(*N*(H)dpa)Cl]Cl	Pt(*N*(H)dpa)(5′-GMP)[a]
C6/6′	150.4	150.4
		150.0
		149.9
C5/5′	126.6	126.9
		126.8
C4/4′	142.5	142.8
C3/3′	124.1	124.3
C2/2′	167.5	167.2
C7/7′	60.79	60.83
		60.77

[a]C8: 141.0 (anti), 141.6 (syn), and 138.8 ppm (free); C1′: 89.72 (anti), 89.76 (syn), and 88.21 ppm (free); C2′: 75.98 and 75.80, 75.22 ppm (free).

into the same narrow shift region as the H3/3′ doublets, and as many as four signals could conceivably be resolved for each type of proton in the Pt(*N*(H)dpa)(**G**) adducts. Shifts of the ^{13}C NMR signals of C6/6′ and C3/3′ are likely to be in distinctive widely dispersed regions for both the simpler [Pt(*N*(H)dpa)Cl]$^+$ complex and the Pt(*N*(H)dpa)(5′-GMP) adduct; therefore, we elected to use HSQC spectroscopy to assign the [Pt(*N*(H)dpa)Cl]$^+$ ^{13}C NMR signals and to use these shifts as a guide in assigning the Pt(*N*(H)dpa)(5′-GMP) ^{13}C NMR signals.

[Pt(*N*(H)dpa)Cl]Cl Assignments. The pyridyl ^{1}H NMR signals for [Pt(*N*(H)dpa)Cl]$^+$ (H6/6′, H5/5′, H4/4′, and H3/3′) are shown in Figure 4. The H6/6′ signal must be a doublet and also the most downfield pyridyl signal because of the proximity of the H6/6′ protons to the endocyclic nitrogen. The difference in coupling constants for the H6/6′ doublet (J = 5.8 Hz) and the more upfield H3/3′ doublet (J = 8.0 Hz) allows assignments of the two pyridyl triplets: the triplet at 7.98 ppm with J = 8.0, ∼7.7 Hz is H4/4′, and the triplet at 7.34 ppm with J = 5.8, ∼7.7 is H5/5′. After the proton assignments of [Pt(*N*(H)dpa)Cl]$^+$ were confirmed with a COSY experiment, the ^{13}C NMR signals of [Pt(*N*(H)dpa)Cl]$^+$ were assigned through an HSQC experiment (Table 3, Figure S1, Supporting Information). An HSQC cross-peak from the H6/6′ signal at 8.61−150.4 ppm assigns the C6/6′ ^{13}C NMR signal. Cross-peaks to the H3/3′ (7.48−124.1 ppm), H4/4′ (7.98−142.5 ppm), and H5/5′ (7.34−126.6 ppm) signals assign the C3/3′, C4/4′, and C5/5′ signals, respectively. Cross-peaks from the H7/7′ signals at 4.73 and 4.49 ppm to the ^{13}C NMR signal at 60.79 ppm assign the C7/7′ signal. The 1D ^{13}C NMR spectrum (shown in Figure S1, Supporting Information, and used for obtaining more precise shifts) reveals that the C2/2′ signal (with no HSQC cross-peak) is the most downfield ^{13}C NMR signal (Table 3), as expected from its proximity to the pyridyl nitrogen.

For [Pt(*N*(H)dpa)Cl]Cl, the C7 and C7′ methylene groups are equivalent, but in each the protons are not equivalent and are designated as *endo*-CH and *exo*-CH protons, respectively (Figure 5). From the Karplus equation, the N−H−C−H coupling constant should be larger for the *endo*-CH signal than for the *exo*-CH signal, owing to the larger dihedral angle between the N−H and the *endo*-CH protons. Because N−H exchange with D_2O occurs in the D_2O/DMSO-d_6 mixture, a ^{1}H NMR spectrum of [Pt(*N*(H)dpa)Cl]Cl in DMSO-d_6 was

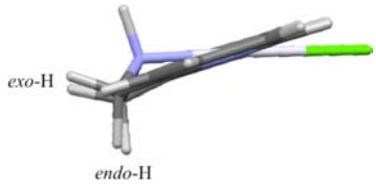

Figure 5. Orientation of the pyridyl rings in the [Pt(*N*(H)dpa)Cl]$^+$ cation, viewed along the coordination plane. Also shown, the designation of the *endo*-CH and the *exo*-CH protons.

recorded. The downfield H7/7′ signal at 4.92 ppm has a higher N−H−C−H coupling constant (8.9 Hz) and is assigned to *endo*-CH. The upfield H7/7′ signal at 4.60 ppm (5.1 Hz) is assigned to *exo*-CH. Thus, in the ^{1}H NMR spectrum of [Pt(*N*(H)dpa)Cl]Cl in D_2O/DMSO-d_6, we assign the downfield H7/7′ signal at 4.73 ppm to *endo*-CH and the upfield H7/7′ signal at 4.49 ppm to *exo*-CH.

Pt(*N*(H)dpa)(5′-GMP) Adduct. The reaction of [Pt(*N*(H)dpa)Cl]$^+$ with 2.5 molar equiv of 5′-GMP was monitored in D_2O/DMSO-d_6 by ^{1}H NMR spectroscopy at 10 min, 7 h, and 49 h after mixing. Even at 10 min, the spectrum (Figure S2, Supporting Information) exhibited two small, sharp, downfield singlets. These singlets provide evidence for restricted rotation of the adduct and clearly belong to H8, the only type of aromatic proton in the reaction mixture (Figure 1) that can give a singlet signal. The large downfield shift change of the product H8 singlets, relative to the free 5′-GMP H8 singlet at 7.96 ppm, can be explained only by coordination of the 5′-GMP to Pt(II) via N7. The singlets at 9.08 and 8.72 ppm (Figure 4) are assigned to the anti and syn rotamers (Figure 3), respectively (see below). The H1′ doublets of the rotamers are also in a quite distinctive region (∼5.9−6.0 ppm); these signals are shifted downfield of the H1′ doublet of free 5′-GMP at 5.71 ppm (Table 1 and Figure S2, Supporting Information). As commonly observed, the inductive effect of the Pt(II) shifts the H8 and H1′ signals of Pt(L)(5′-GMP) adducts downfield compared to these signals for free 5′-GMP.[43−45,52]

Two downfield H8 singlets were found for all of the Pt(*N*(H)dpa)(**G**) adducts (see below). Thus, **G** base rotation about the Pt−N7 bond is impeded in all adducts. We attribute the cause of this restricted rotation to steric impedance of nucleobase rotation by the H6/6′ protons, which are in a fixed position projecting toward the coordinated **G** nucleobase. However, the shift difference between the two H8 signals, $\Delta\delta$, is ∼0.36 ppm, considerably larger than the typical value, such as $\Delta\delta$ = 0.04 found for Pt(Me$_5$dien)(5′-GMP).[44] The pyridyl rings of the Pt(*N*(H)dpa) moiety do not lie exactly in the coordination plane (Figure 5), and the plane of the **G** nucleobase in adducts lies more or less perpendicular to the planes of the pyridyl rings and to the coordination plane. In the syn rotamer, the shielding region of the pyridyl rings projects over the guanine H8; hence, the syn H8 signal will be shifted upfield from the anti H8 signal because of the anisotropic effect of the *N*(H)dpa pyridyl rings (Figure 3). Thus, the anisotropy of the pyridyl rings not only explains the large $\Delta\delta$, but also allows us to assign the rotamers by using H8 shifts. These rotamer assignments are also supported by analysis of the relative shifts of the *N*(H)dpa signals as described below.

The ∼1 ppm upfield shift of the H6/6′ signals (Figure 4 and Table 2) is the other large shift change accompanying adduct formation. The upfield shift of the H6/6′ pyridyl signals of *N*(H)dpa upon Pt(*N*(H)dpa)(5′-GMP) adduct formation is

dx.doi.org/10.1021/ic3018634 | Inorg. Chem. 2012, 51, 11961−11970

similar to that of the H6/6′ signals (~1.0−1.4 ppm) accompanying formation of Pt(5,5′-Me_2Bipy)(5′-GMP)$_2$ from the starting complex, Pt(5,5′-Me_2Bipy)Cl_2 (5,5′-Me_2Bipy = 5,5′-dimethylbipyridine).[35] For both types of adducts, the H6/6′ protons have a similar relationship to the guanine nucleobase.

In contrast to the H6/6′ protons, the H3/3′ protons are the pyridyl protons of the Pt(*N*(H)dpa)(5′-GMP) adduct farthest from the coordinated guanine nucleobase. Thus, the H3/3′ doublets of the adduct should have shifts (~7.50 ppm) similar to that of the H3/3′ signal of the starting [Pt(*N*(H)dpa)Cl]$^+$ complex. As a result, the H3/3′ and the H6/6′ doublets of the Pt(*N*(H)dpa)(5′-GMP) adduct have similar shifts (Table 2). An additional complicating feature in making *N*(H)dpa assignments is the fact that the Pt(*N*(H)dpa)(5′-GMP) adduct has no mirror plane because of the chiral sugar group; thus, the left and right sides of the *N*(H)dpa carrier ligand are magnetically inequivalent for both rotamers. Hence, each rotamer could have two ^{1}H NMR signals for each type of pyridyl proton, raising the possibility that four signals could be resolved for each type of pyridyl proton, for example, four H6/6′ signals in a spectrum of a given adduct.

Therefore, as mentioned, assigning which signals are H3/3′ doublets and which signals are H6/6′ doublets in a crowded spectral region with overlapping signals is difficult on the basis of ^{1}H NMR shift values alone. We relied on [Pt(*N*(H)dpa)Cl]$^+$ assignments to make the ^{1}H and ^{13}C NMR assignments for the Pt(*N*(H)dpa)(5′-GMP) adduct (Figure 6, Tables 2 and 3). The

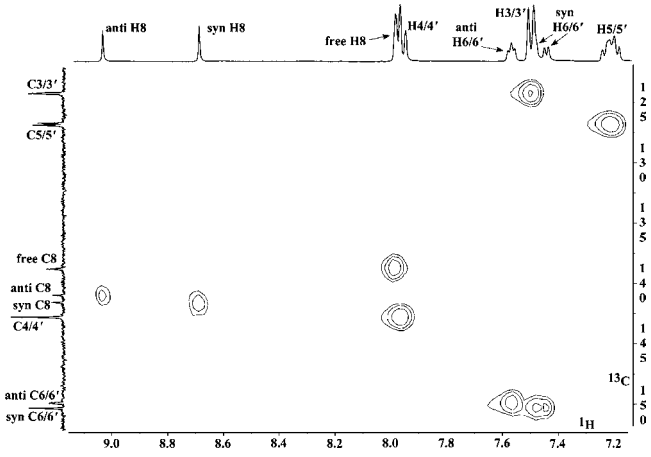

Figure 6. HSQC spectrum of the aromatic region of the Pt(*N*(H)-dpa)(5′-GMP) adduct (shifts in ppm).

1D carbon spectrum shows three resolved C6/6′ peaks at 150.4, 150.0, and 149.9 ppm. In the HSQC spectrum of the Pt(*N*(H)dpa)(5′-GMP) adduct, three closely spaced ^{1}H6/6′-^{13}C6/6′ cross-peaks have a characteristic carbon shift of ~150.0 ppm. One cross-peak involves the quasi-triplet at 7.57 ppm and the two C6/6′ peaks at 150.0 and 149.9 ppm; these signals are attributable to the anti rotamer. The other two cross-peaks involve the two doublets at 7.51 and 7.44 ppm and the single C6/6′ peak at 150.4 ppm; these signals are attributable to the syn rotamer. The C3/3′ pyridyl signal of the Pt(*N*(H)-dpa)(5′-GMP) adduct at a characteristic shift (124.3 ppm) has a cross-peak with the broad doublet peak at 7.51 ppm; this cross-peak arises from overlapped H3/3′ and C3/3′ signals of the syn and anti rotamers. This 7.51 ppm peak also has a cross-peak to the syn C6/6′ peak, indicating that this peak also contains one syn H6/6′ signal. In summary, the assignment of the four H6/6′ signals involves the quasi-triplet (containing two overlapped anti H6/6′ doublets) at 7.57 ppm, the syn H6/6′ signal overlapped with the H3/3′ doublets at 7.51 ppm, and the syn H6/6′ doublet at 7.44 ppm.

The H5/5′ quasi-quartet at 7.21 ppm has a single elongated cross-peak to the C5/5′ pyridyl signals of the Pt(*N*(H)dpa)(5′-GMP) adduct at a characteristic shift [126.8 and 126.9 ppm], indicating that the signals attributable to each rotamer have slightly different chemical shifts, forming a quasi-quartet. Assigning the H5/5′ signals specifically to the syn or anti rotamer is difficult to assess because these signals overlap. The C4/4′ pyridyl signal of the Pt(*N*(H)dpa)(5′-GMP) adduct at a characteristic shift (142.8 ppm) has a cross-peak with the overlapped triplets at 7.97 ppm, thus assigning the peak to H4/4′ signals from both rotamers. Two C7/7′ peaks at 60.83 and 60.77 ppm in the 1D ^{13}C NMR spectrum have cross-peaks to the cluster of H7/7′ signals at 4.80 ppm and to the suppressed H7/7′ signals overlapped with the HOD solvent peak at 4.57 ppm (Figure S3, Supporting Information).

A comparison of *J* values for the H6/6′ and H3/3′ signals of [Pt(*N*(H)dpa)Cl]$^+$ (5.8 and 8.0 Hz, respectively, Table 2) with those for the Pt(*N*(H)dpa)(5′-GMP) adduct was used to support the assignments of the rotamer signal types. The two H6/6′ peaks (the quasi-triplet and the upfield doublet) both had *J* ~5.4 Hz, values consistent with the expected H6/6′ *J* value (Table 2). The *J* value (~8.0 Hz) for the H3/3′ signal (broad doublet) is also consistent with the value expected for an H3/3′ signal (Table 2).

A ROESY experiment allowed us to assign the H6/6′ signals specifically to syn and anti Pt(*N*(H)dpa)(5′-GMP) rotamers because the *N*(H)dpa H6/6′ protons are close to the 5′-GMP H8 protons in both Pt(*N*(H)dpa)(5′-GMP) rotamers. Thus, H8-to-H6/6′ NOE cross-peaks were expected. The ROESY spectrum (Figure 7) showed a very intense cross-peak from the

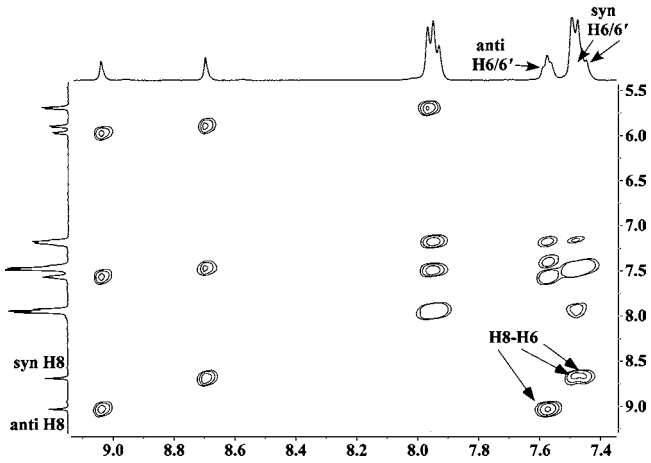

Figure 7. ^{1}H-^{1}H ROESY spectrum of the aromatic region of the Pt(*N*(H)dpa)(5′-GMP) adduct (shifts in ppm).

anti H8 signal to the quasi-triplet (a peak composed of two overlapping downfield H6/6′ doublets). The syn H8 signal had cross-peaks to the most upfield H6/6′ doublet and to the H6/6′ signal that overlaps with the H3/3′ signal. These findings confirm that the most downfield H6/6′ peak is composed of the two H6/6′ signals from the anti rotamer and that the two H6/6′ signals of the syn rotamer are relatively upfield. The

dx.doi.org/10.1021/ic3018634 | *Inorg. Chem.* 2012, 51, 11961−11970

relationships of these shifts to the structure of the rotamers are explained next.

The relative values of large upfield shift changes of the H6/6′ signals on formation of the Pt(*N*(H)dpa)(5′-GMP) adduct arising from the anisotropy of the guanine nucleobase provide confirmation of our assignment of the rotamers. The Pt−N7 bond restricts how closely the five-membered ring can approach the H6/6′ protons as the nucleobase wags back and forth from thermal motion. The H6/6′ protons are not in the coordination plane (Figure 5), as mentioned above. The nucleobase H8 proton is closer to the H6/6′ protons in the anti rotamer, and this restricts the degree of base wagging because the partial positive charge of these protons leads to mutual electrostatic repulsion. In addition, the H6/6′ protons and the six-membered ring are on opposite sides of the coordination plane. Thus, as suggested in Figure 8, the nucleobase in the anti

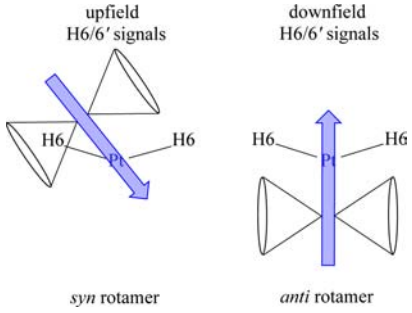

Figure 8. Possible orientations of the guanine base represented by an arrow. The anisotropy is indicated by cones emanating from the six-membered ring. Illustrated is the proximity of the six-membered ring to the H6/6′ protons in the syn rotamer, resulting in a more upfield shift of the H6/6′ signals of the syn rotamer compared to the anti rotamer, in which the six-membered ring is farther away from the H6/6′ protons.

rotamer is probably not tilted on average. Overlap of the two anti H6/6′ doublets (appearing as a quasi-triplet) at 7.57 ppm results from the similar environments of the two H6/6′ protons; the environments are similar because the anti H6/6′ protons are relatively far from the six-membered ring (Figure 8), the smaller anisotropic effects lead to similar shifts for the two H6/6′ signals and result in a relatively downfield pair of overlapping signals. For the syn rotamer, H8 is on the side of the coordination plane opposite to the H6/6′ protons. Thus, base tilting is not hindered by H8-to-H6/6′ electronic repulsion. Wagging leads to a closer proximity of the nucleobase anisotropic six-membered ring to the H6/6′ protons of the syn rotamer than of the anti rotamer (Figure 8), accounting for the more upfield shift of the syn H6/6′ signals than the anti H6/6′ signals.

The above interpretations of shift relationships are consistent in all adducts studied here and also with the conclusion reached by using the H8 signals. Furthermore, the H8 and H1′ protons are both associated with the five-membered ring of the guanine base. Thus, the syn H8 and H1′ signals are affected by the anisotropy of the pyridyl rings in a similar manner: both have H8 and H1′ signals with shifts upfield from those of the anti rotamer.

Anisotropy can be used to analyze the small shift changes found for the Pt(*N*(H)dpa)(5′-GMP) H4/4′ and H5/5′ triplets, which are expected to have similar chemical shifts for both rotamers. Because the H4/4′ pyridyl protons are positioned away from the coordinated 5′-GMP site, no significant shift change takes place; therefore, we can assign the most downfield broad triplet at 7.97 ppm to the H4/4′ signals for both rotamers. The H5/5′ protons are the second-closest pyridyl protons to the 5′-GMP nucleobase. Thus, owing to the anisotropy of the six-membered ring of the guanine base, the H5/5′ triplets are shifted upfield, as compared to the H5/5′ triplet of the starting $[Pt(N(H)dpa)Cl]^+$ complex. The H5/5′ peak of the adduct appears as a distorted quartet attributable to overlapping signals of the syn and anti rotamers.

The methylene protons (H7/7′) are far from the nucleobase and were not assigned to a particular rotamer, mainly because of close overlap of the syn and anti rotamers. The methylene signals reside in the same region as the HOD solvent peak. Presaturation of the HOD signal precludes using the NOE cross-peaks to assess the *endo*-CH and *exo*-CH signals. However, we can confidently assign the cluster of downfield signals at 4.80 ppm to the *endo*-CH protons and the suppressed signals at 4.57 ppm to the *exo*-CH protons because the downfield H7/7′ signal of [Pt(*N*(H)dpa)Cl]Cl is the *endo*-CH signal, as discussed above.

Pt(*N*(H)dpa)(5′-GTP) and Pt(*N*(H)dpa)(5′-GDP). In past work, rotamer distribution was found to be influenced by H-bonding interactions between phosphate and N−H groups. In addition, either the N−H group was cis to **G** in an amine ligand of Pt(L)(**G**) and Pt(L)$(\mathbf{G})_2$ adducts or the **G** N1−H group was on an adjacent cis **G** residue in Pt(L)$(\mathbf{G})_2$ adducts.[34,38−41,70−72] Because the adducts investigated here have only one **G** and no N−H protons cis to this **G**, the Pt(*N*(H)dpa)(**G**) adducts offer the opportunity to assess the role of a trans N−H group in influencing rotamer abundance. Toward this goal, adducts of 5′-GTP and 5′-GDP were compared to the Pt(*N*(H)dpa)(5′-GMP) adduct, for which the ratio of the two rotamers was ∼1:1 (Table 4). In Pt(*N*(H)dpa)(5′-GTP), the long triphosphate

Table 4. Anti H8:Syn H8 Intensity Ratios for Pt(*N*(H)dpa)(G) Adducts

G	pH	anti:syn ratio
5′-GMP	4.0	1:1.14
5′-GDP	4.1	1:1.04
	7.5[a]	1:1.05
5′-GTP	2.7[b]	1:1.04
	4.1	1.22:1
	7.3[c]	1.37:1
5′-IMP[d]	4.0	1:1.25
Guo	4.1	1:1.34
9-EtG	4.1	1:1.28

[a]H8: 9.15 (anti), and 8.79 ppm (syn). [b]H8: 9.16 (anti), and 8.75 ppm (syn). [c]H8: 9.22 (anti), and 8.79 ppm (syn). [d]H2: anti H2:syn H2 ratio (1.21:1).

chain of the 5′-GTP can extend far enough for the γ-phosphate group to form a hydrogen bond with the trans N−H of the carrier ligand when the 5′-GTP nucleotide has the anti conformation (Figure 9). Such hydrogen bonding would increase the abundance of the anti rotamer. However, such hydrogen bonding would not occur for the 5′-GDP adduct because the diphosphate chain is too short to reach the trans N−H.

The reactions of $[Pt(N(H)dpa)Cl]^+$ with 2.5 molar equiv of 5′-GDP or 5′-GTP were essentially complete in one to two days at pH ∼4.1. For both adducts, sharp product H8 singlets

dx.doi.org/10.1021/ic3018634 | *Inorg. Chem.* 2012, 51, 11961−11970

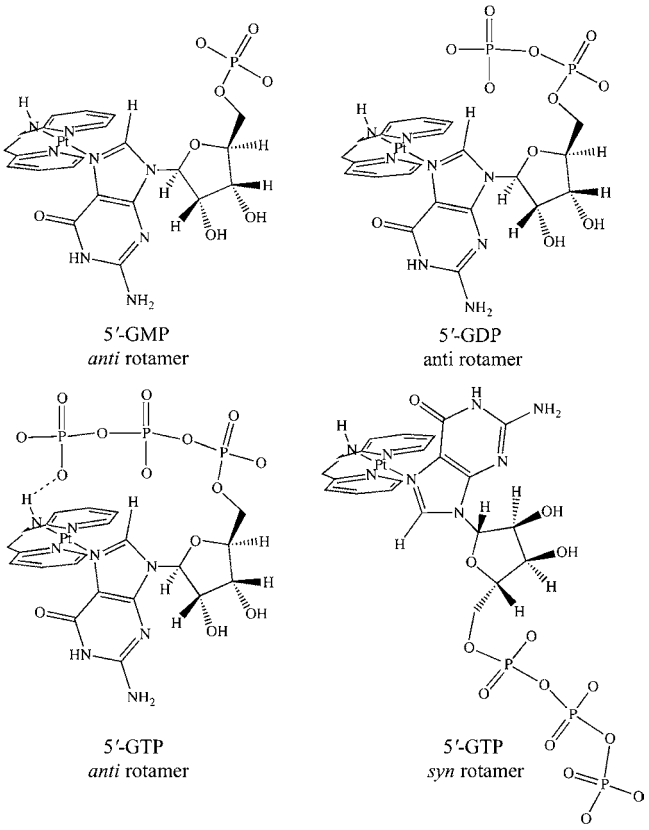

Figure 9. Proposed hydrogen bonding of the γ-phosphate group of 5′-GTP with the N−H in the anti rotamer of the Pt(*N*(H)dpa)(5′-GTP) adduct (*lower left*). The figure also illustrates that the distance between the N−H group and the closest phosphate group is too long to support hydrogen bonding in the corresponding syn 5′-GTP rotamer (*bottom right*) and in the anti rotamers of the 5′-GMP and 5′-GDP adducts (*top*).

were observed for the anti rotamer (the downfield H8 and H1′ signals) and the syn rotamer (the upfield H8 and H1′ signals) (Figure 10, Tables 1 and 2, Figure S4, Supporting Information). For the Pt(*N*(H)dpa)(5′-GTP) solution at pH 4.1, the anti H8:syn H8 ratio was 1.22:1 (Table 4); this is the only adduct having an anti H8:syn H8 ratio greater than one. The slightly larger value of $\Delta\delta$ ~0.42 ppm for the 5′-GTP rotamers than for the 5′-GMP rotamers (Table 1) is accounted for by the deshielding of H8 by the overhanging phosphate groups of 5′-GTP. This chain should be close to H8 when a hydrogen bond is formed between the phosphate chain and the central *N*(H)dpa N−H group in the anti rotamer (Figure 9). The H8 signal of the syn rotamer shows a similar downfield shift compared to that of the 5′-GMP adduct (Table 1) mainly because the phosphate chain has more conformational freedom in the absence of an H-bond interaction (Figure 9). The *N*(H)dpa aromatic signals in the Pt(*N*(H)dpa)(5′-GTP) adduct have shifts similar to those of the 5′-GMP adduct (Table 2 and Figure S5, Supporting Information).

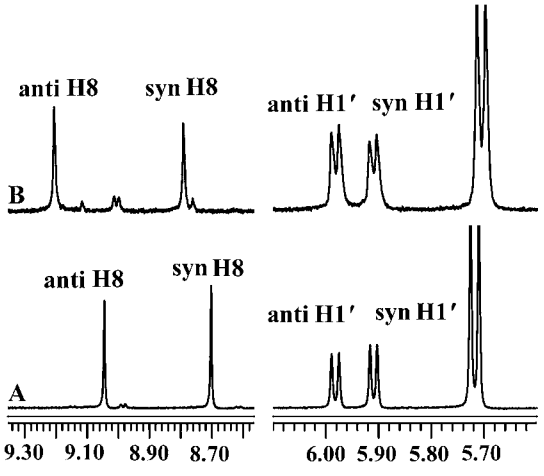

Figure 10. H8 and H1′ regions of the ^{1}H NMR spectra of the Pt(*N*(H)dpa)(5′-GMP) adduct (A) and the Pt(*N*(H)dpa)(5′-GTP) adduct (B) (shifts in ppm). The H1′ doublet of the free nucleotide is also shown at ~5.7 ppm.

In the ROESY spectrum of the Pt(*N*(H)dpa)(5′-GTP) adduct (Table 2 and Figure S6, Supporting Information), the anti H8 signal has a cross-peak to the most downfield H6/6′ signal, which contains two H6/6′ signals overlapping as a broad doublet, assigning both downfield H6/6′ signals to the anti rotamer. The syn H8 signal has cross-peaks to the H6/6′ signal overlapped with the H3/3′ signal and to the most upfield H6/6′ signal, thus assigning these two H6/6′ signals to the syn rotamer.

To obtain further evidence that the anti rotamer of Pt(*N*(H)dpa)(5′-GTP) has a hydrogen bond from the γ-phosphate to the central N−H, the pH of the solution was raised to deprotonate more fully the γ-phosphate group, favoring hydrogen bonding and thereby increasing the abundance of the anti rotamer. When the pH was raised from 4.1 to 7.3, the anti H8:syn H8 ratio increased from 1.22:1 to 1.37:1 (Table 4). On the other hand, when the pH was lowered to 2.7, the ratio decreased to 1:1.04, and some signals shifted noticeably (Table 4). The Pt(*N*(H)dpa)(5′-GDP) adduct was used as a "control" because models suggest that the diphosphate chain of 5′-GDP is too short to form a hydrogen bond. For Pt(*N*(H)dpa)(5′-GDP) solutions at pH 4.1 and 7.5, the anti H8:syn H8 ratio was essentially unchanged at ~1:1. This adduct, like all other adducts except Pt(*N*(H)-dpa)(5′-GTP), favors the syn rotamer. These findings and the relatively downfield H8 signal of the Pt(*N*(H)dpa)(5′-GTP) anti rotamer provide evidence for a hydrogen bond between the γ-phosphate and the *N*(H)dpa N−H of this adduct.

Pt(*N*(H)dpa)(5′-IMP). The reaction of [Pt(*N*(H)dpa)Cl]$^+$ with 5′-IMP (molar ratio = 1:2.5) was complete after 50 h (Figure S7, Supporting Information). The Pt(*N*(H)dpa)(5′-IMP) adduct provides another approach for confirming the assignment of rotamer signals because the proton of the six-membered ring of the hypoxanthine base has a signal that can be affected by the pyridyl ring anisotropy. For a given rotamer, the H2 and H8 signals are influenced in an opposite manner by this anisotropy. The H8 singlets for the two rotamers are at 9.44 (anti) and 9.09 (syn) ppm, with an anti H8:syn H8 intensity ratio of 1:1.25 (Figure 11, Table 4). The H2 signals were shifted downfield to 8.26 (syn) and 8.17 (anti) ppm from the H2 signal of free 5′-IMP at 8.05 ppm. The relationship of the signals agrees with the prediction based on the effects of pyridyl ring anisotropy, thus confirming the assignments of the anti and syn rotamer signals. The *N*(H)dpa aromatic signals of the Pt(*N*(H)dpa)(5′-IMP) adduct exhibit a pattern of shift changes very similar to that observed for other adducts (Table 2). However, the syn H6/6′ signal does not overlap with the H3/3′ signal. Hence both H6/6′ signals for the syn rotamer are resolved (Table 2).

dx.doi.org/10.1021/ic3018634 | *Inorg. Chem.* 2012, 51, 11961−11970

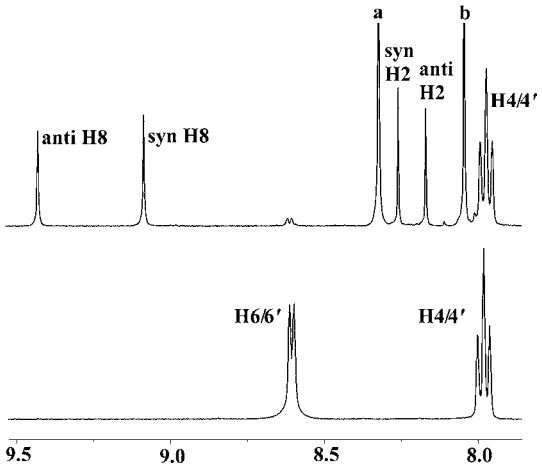

Figure 11. ^{1}H NMR spectra (25 °C, D_2O/DMSO-d_6) of [Pt(*N*(H)dpa)Cl]$^+$ (*bottom*) and of the Pt(*N*(H)dpa)(5′-IMP) adduct (*top*) (shifts in ppm). The spectral region was selected to show the H8 and H2 signals, which for free 5′-IMP are respectively labeled a and b.

[Pt(*N*(H)dpa)(Guo)]$^{2+}$. The large $\Delta\delta$ between the H8 signals of the syn and anti rotamers of the nucleotide adducts could be the result of different anisotropic effects of the phosphate groups in the two rotamers; to assess this possibility, we prepared the [Pt(*N*(H)dpa)(Guo)]$^{2+}$ adduct.

After the reaction of [Pt(*N*(H)dpa)Cl]$^+$ with Guo (molar ratio = 1:2.5) was complete (Figure S8, Supporting Information), the two sharp H8 signals (anti H8:syn H8 ratio = 1:1.34, Table 4) had a $\Delta\delta$ value of ∼0.34 ppm, about the same as observed for the 5′-GMP adduct. These results indicate that phosphate groups at the 5′ position have at best a small influence on $\Delta\delta$ and on impeding nucleobase rotation. The *N*(H)dpa signals were assigned by comparison to the shift values for the nucleotide adducts (Table 2).

[Pt(*N*(H)dpa)(9-EtG)]$^{2+}$. To definitively exclude the possibility that the sugar moiety could be contributing to the large $\Delta\delta$ and to the slow nucleobase rotation of the adducts described above, we explored the properties of the [Pt(*N*(H)dpa)(9-EtG)]$^{2+}$ adduct, which has a small alkyl group in place of the sugar.

After the reaction was complete (Figure S9, Supporting Information), two sharp H8 ^{1}H NMR signals (Table 1) had a $\Delta\delta$ of 0.33 ppm, indicating slow rotation around the Pt−N7 bond. Thus, the sugar residue is not responsible for the slow rotation, nor for the large $\Delta\delta$ observed. The anti H8:syn H8 intensity ratio is 1:1.28 (Table 4). Correlating the abundance of the two sets of CH_2 and CH_3 signals with that of the H8 signals establishes that the anti rotamer has the more downfield signals for all of the protons associated with the five-membered guanine ring (Table 1).

Because of the absence of the chiral sugar group, only one signal for each pyridyl proton type was observed for each rotamer. The pyridyl signals of the [Pt(*N*(H)dpa)(9-EtG)]$^{2+}$ adduct have shifts very similar to those of the corresponding signals of the [Pt(*N*(H)dpa)(Guo)]$^{2+}$ adduct (Table 2).

Other Information Derived from the NMR Data. The observation of H8−H1′ cross-peaks having an equal intensity for both the syn and anti rotamers indicates that the nucleotide in both rotamers has conformational freedom and that syn and anti nucleotide conformations coexist. Because of the high concentration of 5′-GMP anion in the reaction mixture, stacking interactions between the 5′-GMP base and the pyridyl rings of positively charged [Pt(*N*(H)dpa)Cl]$^+$ starting material cause a similar upfield shifting of all of the pyridyl signals immediately after the addition of 5′-GMP. For example, the H6/6′ signal (Figure S10, Supporting Information) of the starting complex is shifted upfield by 0.08 ppm. As the reaction progressed, the concentration of 5′-GMP decreased, and the resulting decrease in the stacking interaction caused the H6/6′ signal of [Pt(*N*(H)dpa)Cl]$^+$ to shift downfield toward its original value prior to 5′-GMP addition. All of the other adducts with an anionic **G** (**G** = 5′-GDP, 5′-GTP, 5′-IMP) showed a similar upfield shift of the pyridyl signals of the starting complex upon addition of **G**, as observed for the 5′-GMP adduct. However, when 9-EtG (an N9 guanine derivative) was added, no upfield shifting was observed for the [Pt(*N*(H)dpa)Cl]$^+$ signals.

CONCLUSIONS

Two sharp ^{1}H NMR H8 signals observed for all Pt(*N*(H)dpa)(**G**) adducts studied here (**G** = 5′-GMP, 5′-GDP, 5′-GTP, Guo, 9-EtG, and 5′-IMP) provided evidence that they all exist as interconverting mixtures of syn and anti rotamers. The bulk of the tridentate *N*(H)dpa carrier ligand is sufficient to impede the rotation of **G** about the Pt−N7 bond for these adducts. We conclude that the close proximity of the anisotropic pyridyl rings of *N*(H)dpa in Pt(*N*(H)dpa)(**G**) adducts to the H8 of the nucleobase accounts for the large $\Delta\delta$ observed for all adducts. From NMR data, we conclude that the pyridyl H6/6′ atoms strongly impede the rotation of **G** in these adducts. The ^{1}H NMR spectra of these Pt(*N*(H)dpa)(**G**) adducts had four potentially resolvable H6/6′ signals because the chiral sugar group makes the left and right sides of *N*(H)dpa magnetically inequivalent for both rotamers. In the syn rotamer of Pt(*N*(H)dpa)(**G**), the relative proximity of the six-membered ring of **G** to the H6/6′ pyridyl protons accounts for the upfield shift observed for these resonances compared to those of the anti rotamer. Tilting of **G** occurs in each of the rotamers, but a more noticeable effect is seen in the syn rotamer because of the larger chemical shift difference between the two H6/6′ signals for the syn rotamer, indicating that **G** is tilted, with the six-membered ring closer to one H6/6′ proton than the other. Evidence was observed for a weak hydrogen bond between the γ-phosphate group of 5′-GTP and the central N−H of the carrier ligand in the Pt(*N*(H)dpa)(5′-GTP) adduct. From results for the [Pt(*N*(H)dpa)(9-EtG)]$^{2+}$ adduct, we concluded that the guanine base alone, not the sugar or phosphate group, slowed the rate of nucleobase rotation about the Pt−N7 bond in nucleotide adducts. [Pt(*N*(H)dpa)Cl]Cl and its analogues should have enough bulk to be anticancer active; however, further studies will be necessary to evaluate their potential anticancer properties.

ASSOCIATED CONTENT

Supporting Information

^{1}H-^{13}C HSQC spectra of [Pt(*N*(H)dpa)Cl]Cl and the Pt(*N*(H)dpa)(5′-GMP) adduct; ^{1}H NMR stack plots of the reaction forming the Pt(*N*(H)dpa)(5′-GMP), Pt(*N*(H)dpa)(5′-GDP), Pt(*N*(H)dpa)(5′-GTP), Pt(*N*(H)dpa)(5′-IMP), [Pt(*N*(H)dpa)(Guo)]$^{2+}$, and [Pt(*N*(H)dpa)(9-EtG)]$^{2+}$ adducts; ROESY spectrum of the aromatic region of the Pt(*N*(H)dpa)(5′-GTP) adduct; and ^{1}H NMR stack plot showing the shifting of the [Pt(*N*(H)dpa)Cl]$^+$ H6/6′ signal from the stacking interaction between the pyridyl rings of

dx.doi.org/10.1021/ic3018634 | *Inorg. Chem.* 2012, 51, 11961−11970

[Pt(*N*(H)dpa)Cl]$^+$ and the 5′-GMP base in the Pt(*N*(H)dpa)-(5′-GMP) adduct reaction. This material is available free of charge via the Internet at http://pubs.acs.org.

AUTHOR INFORMATION

Corresponding Author

*E-mail: lmarzil@lsu.edu.

Notes

The authors declare no competing financial interest.

ACKNOWLEDGMENTS

Instrumentation used in this study was supported by NSF Grant 0421356. We thank Dr. W. Dale Treleaven for his help in obtaining some of the ROESY spectra on the DPX spectrometer (400 MHz).

REFERENCES

(1) Arnesano, F.; Natile, G. *Coord. Chem. Rev.* **2009**, *253*, 2070−2081.
(2) Kelland, L. *Nature (London)* **2007**, *7*, 573−584.
(3) Klein, A. V.; Hambley, T. W. *Chem. Rev.* **2009**, *109*, 4911−4920.
(4) Reedijk, J. *Eur. J. Inorg. Chem.* **2009**, *2009*, 1303−1312.
(5) Jakupec, M. A.; Galanski, M.; Arion, V. B.; Hartinger, C. G.; Keppler, B. K. *Dalton Trans.* **2008**, 183−194.
(6) Ober, M.; Lippard, S. J. *J. Am. Chem. Soc.* **2008**, *130*, 2851−2861.
(7) Hostetter, A. A.; Osborn, M. F.; DeRose, V. J. *Chem. Biol.* **2012**, *7*, 218−225.
(8) Wilson, J. J.; Lippard, S. J. *J. Med. Chem.* **2012**, *55*, 5326−5336.
(9) Liskova, B.; Zerzankova, L.; Novakava, O.; Kostrhunova, H.; Travnicek, Z.; Brabec, V. *Chem. Res. Toxicol.* **2012**, *25*, 500−509.
(10) Yin, R.; Gou, S.; Liu, X.; Lou, L. *J. Inorg. Biochem.* **2011**, *105*, 1095−1101.
(11) Sun, Y.; Gou, S.; Yin, R.; Jiang, P. *Eur. J. Inorg. Chem.* **2011**, *46*, 5146−5153.
(12) Saad, J. S.; Natile, G.; Marzilli, L. G. *J. Am. Chem. Soc.* **2009**, *131*, 12314−12324.
(13) Zoldakova, M.; Beirsack, B.; Kostrhunova, H.; Ahmad, A.; Padhye, S.; Sarkar, F. H.; Schobert, R.; Brabec, V. *Med. Chem. Commun.* **2011**, *2*, 493−499.
(14) Todd, R. C.; Lippard, S. J. *J. Inorg. Biochem.* **2010**, *104*, 902−908.
(15) Malina, J.; Novakava, O.; Vojtiskova, M.; Natile, G.; Brabec, V. *Biophys. Chem.* **2007**, *93*, 3950−3962.
(16) Kasparkova, J.; Vojtiskova, M.; Natile, G.; Brabec, V. *Chem.—Eur. J.* **2008**, *14*, 1330−1341.
(17) Bhattacharyya, D.; Marzilli, P. A.; Marzilli, L. G. *Inorg. Chem.* **2005**, *44*, 7644−7651.
(18) Ohndorf, U.-M.; Rould, M. A.; He, Q.; Pabo, C. O.; Lippard, S. J. *Nature* **1999**, *399*, 708−712.
(19) Marzilli, L. G.; Saad, J. A.; Kuklenyik, Z.; Keating, K. A.; Xu, Y. *J. Am. Chem. Soc.* **2001**, *123*, 2764−2770.
(20) Sullivan, S. T.; Saad, J. S.; Fanizzi, F. P.; Marzilli, L. G. *J. Am. Chem. Soc.* **2002**, *124*, 1558−1559.
(21) Lovejoy, K. S.; Todd, R. C.; Zhang, S.; McCormick, M. S.; D'Aquino, J. A.; Reardon, J. T.; Sancar, A.; Giacomini, K. M.; Lippard, S. J. *Proc. Natl. Acad. Sci.* **2008**, *105*, 8902−8907.
(22) Todd, R. C.; Lippard, S. J. In *Platinum and Other Heavy Metal Compounds in Cancer Chemotherapy*; Bonetti, A., Leone, R., Muggia, F. M., Howell, S. B., Eds.; Humana Press: New York, 2009; pp 67−72.
(23) Hambley, T. W. *J. Chem. Soc., Dalton Trans.* **2001**, 2711−2718.
(24) Beljanski, V.; Villanueva, J. M.; Doetsch, P. W.; Natile, G.; Marzilli, L. G. *J. Am. Chem. Soc.* **2005**, *127*, 15833−15842.
(25) Orbell, J. D.; Taylor, M. R.; Birch, S. L.; Lawton, S. E.; Vilkins, L. M.; Keefe, L. J. *Inorg. Chim. Acta* **1988**, *152*, 125−134.
(26) Benedetti, M.; Malina, J.; Kasparkova, J.; Brabec, V.; Natile, G. *Environ. Health Perspect.* **2002**, *110*, 779−782.
(27) Hirano, T.; Inagaki, K.; Fukai, T.; Alink, M.; Nakahara, H.; Kidani, Y. *Chem. Pharm. Bull.* **1990**, *38*, 2850−2852.
(28) Wang, D.; Zhu, G.; Huang, X.; Lippard, S. J. *Proc. Natl. Acad. Sci.* **2010**, *107*, 9584−9589.
(29) Saad, J. A.; Benedetti, M.; Natile, G.; Marzilli, L. G. *Inorg. Chem.* **2010**, *49*, 5573−5583.
(30) Saad, J. S.; Benedetti, M.; Natile, G.; Marzilli, L. G. *Inorg. Chem.* **2011**, *50*, 4559−4571.
(31) Williams, K. M.; Cerasino, L.; Natile, G.; Marzilli, L. G. *J. Am. Chem. Soc.* **2000**, *122*, 8021−8030.
(32) Ano, S. O.; Intini, F. P.; Natile, G.; Marzilli, L. G. *J. Am. Chem. Soc.* **1998**, *120*, 12017−12022.
(33) Kiser, D.; Intini, F. P.; Xu, Y.; Natile, G.; Marzilli, L. G. *Inorg. Chem.* **1994**, *33*, 4149−4158.
(34) Ano, S. O.; Intini, F. P.; Natile, G.; Marzilli, L. G. *Inorg. Chem.* **1999**, *38*, 2989−2999.
(35) Maheshwari, V.; Marzilli, P. A.; Marzilli, L. G. *Inorg. Chem.* **2008**, *47*, 9303−9313.
(36) Maheshwari, V.; Marzilli, P. A.; Marzilli, L. G. *Inorg. Chem.* **2011**, *50*, 6626−6636.
(37) Sullivan, S. T.; Ciccarese, A.; Fanizzi, F. P.; Marzilli, L. G. *J. Am. Chem. Soc.* **2001**, *123*, 9345−9355.
(38) Saad, J. S.; Scarcia, T.; Natile, G.; Marzilli, L. G. *Inorg. Chem.* **2002**, *41*, 4923−4935.
(39) Wong, H. C.; Intini, F. P.; Natile, G.; Marzilli, L. G. *Inorg. Chem.* **1999**, *38*, 1006−1014.
(40) Sullivan, S. T.; Ciccarese, A.; Fanizzi, F. P.; Marzilli, L. G. *Inorg. Chem.* **2001**, *40*, 455−462.
(41) Carlone, M.; Marzilli, L. G.; Natile, G. *Inorg. Chem.* **2004**, *43*, 584−592.
(42) Carlone, M.; Marzilli, L. G.; Natile, G. *Eur. J. Inorg. Chem.* **2005**, 1264−1273.
(43) Sandlin, R. D.; Starling, M. P.; Williams, K. M. *J. Inorg. Biochem.* **2010**, *104*, 214−216.
(44) Carlone, M.; Fanizzi, F. P.; Intini, F. P.; Margiotta, N.; Marzilli, L. G.; Natile, G. *Inorg. Chem.* **2000**, *39*, 634−641.
(45) Christoforou, A. M.; Marzilli, P. A.; Marzilli, L. G. *Inorg. Chem.* **2006**, *45*, 6771−6781.
(46) Cramer, R. E.; Dahlstrom, P. L. *J. Am. Chem. Soc.* **1979**, *101*, 3679−3681.
(47) Cramer, R. E.; Dahlstrom, P. L. *Inorg. Chem.* **1985**, *24*, 3420−3424.
(48) Cramer, R. E.; Dahlstrom, P. L.; Seu, M. J. T.; Norton, T.; Kashiwagi, M. *Inorg. Chem.* **1980**, *19*, 148−154.
(49) Xu, Y.; Natile, G.; Intini, F. P.; Marzilli, L. G. *J. Am. Chem. Soc.* **1990**, *112*, 8177−8179.
(50) Ndinguri, M. W.; Fronczek, F. R.; Marzilli, P. A.; Crowe, W. E.; Hammer, R. P.; Marzilli, L. G. *Inorg. Chim. Acta* **2010**, *363*, 1796−1804.
(51) Marcelis, A. T. M.; Erkelens, C.; Reedijk, J. *Inorg. Chim. Acta* **1984**, 129−135.
(52) Kong, P.-C.; Theophanides, T. *Bioinorg. Chem.* **1975**, *5*, 51−58.
(53) Benedetti, M.; Ducani, C.; Migoni, D.; Antonucci, D.; Vecchio, V. M.; Ciccarese, A.; Romano, A.; Verri, T.; Ciccarella, G.; Fanizzi, F. P. *Angew. Chem.* **2008**, *120*, 517−520.
(54) Murdoch, P. S.; Guo, Z.; Parkinson, J. A.; Sadler, P. J. *J. Bioinorg. Chem.* **1999**, *4*, 32−38.
(55) Guo, Z.; Sadler, P. J.; Zang, E. *Chem. Commun.* **1997**, 27−28.
(56) Mikola, M.; Klika, K. D.; Hakala, A.; Arpalahti, J. *Inorg. Chem.* **1999**, *38*, 571−578.
(57) Macquet, J.-P.; Butour, J.-L. *Eur. J. Biochem.* **1978**, *83*, 375−387.
(58) Bursova, V.; Kasparkova, J.; Hofr, C.; Brabec, V. *Biophys. J.* **2005**, *88*, 1207−1214.
(59) Horacek, P.; Drobnik, J. *Biochim. Biophys. Acta* **1971**, *254*, 341−347.
(60) Srivastava, R. C.; Froehlich, J. In *Recent Results in Cancer Research. Platinum Coordination Complexes in Cancer Chemotherapy*; Connors, T. A., Roberts, J. J., Eds.; Springer-Verlag: Heidelberg, Germany, 1974; Vol. *48*, pp 75−77.

(61) Marzilli, L. G.; Reily, M. D.; Heyl, B. L.; McMurray, C. T.; Wilson, W. D. *FEBS Lett.* **1984**, *176*, 389−392.
(62) Reily, M. D.; Marzilli, L. G. *J. Am. Chem. Soc.* **1985**, *107*, 4916−4924.
(63) Guney, E.; Yilmaz, V. T.; Ari, F.; Buyukgungor, O.; Ulukaya, E. *Polyhedron* **2011**, *30*, 114−122.
(64) Ulukaya, E.; Ari, F.; Dimas, K.; Sarimahmut, M.; Guney, E.; Sakellaridis, N.; Yilmaz, V. T. *J. Cancer Res. Clin. Oncol.* **2011**, *137*, 1425−1434.
(65) Price, J. H.; Williamson, A. N.; Schramm, R. F.; Wayland, B. B. *Inorg. Chem.* **1972**, *11*, 1280−1284.
(66) Pitteri, B.; Annibale, G.; Marangoni, G.; Bertolasi, V.; Ferretti, V. *Polyhedron* **2002**, *21*, 2283−2291.
(67) Gottleib, H. E.; Kotlyar, V.; Nudelman, A. *J. Org. Chem.* **1997**, *62*, 7512−7515.
(68) van Boom, S. S. G. E.; Chen, B. W.; Tueben, J. M.; Reedijk, J. *Inorg. Chem.* **1999**, *38*, 1450−1455.
(69) Barnham, K. J.; Djuran, M. I.; Murdoch, P. S.; Sadler, P. J. *J. Chem. Soc., Chem. Commun.* **1994**, 721−722.
(70) Natile, G.; Marzilli, L. G. *Coord. Chem. Rev.* **2006**, *250*, 1315−1331.
(71) Benedetti, M.; Tamasi, G.; Cini, R.; Marzilli, L. G.; Natile, G. *Chem.—Eur. J.* **2007**, *13*, 3131−3142.
(72) Williams, K. M.; Cerasino, L.; Intini, F. P.; Natile, G.; Marzilli, L. G. *Inorg. Chem.* **1998**, *37*, 5260−5268.